Annual Review of Analytical Chemistry

Active Flow Control and Dynamic Analysis in Droplet Microfluidics

Nan Shi, Md Mohibullah, and Christopher J. Easley

Department of Chemistry and Biochemistry, Auburn University, Auburn, Alabama 36849, USA; email: chris.easley@auburn.edu

Annu. Rev. Anal. Chem. 2021. 14:133–53

First published as a Review in Advance on May 12, 2021

The *Annual Review of Analytical Chemistry* is online at anchem.annualreviews.org

https://doi.org/10.1146/annurev-anchem-122120-042627

Keywords

microfluidics, droplets, programmable, dynamic analysis, analog and digital information

Abstract

Droplet-based microfluidics has emerged as an important subfield within the microfluidic and general analytical communities. Indeed, several unique applications such as digital assay readout and single-cell sequencing now have commercial systems based on droplet microfluidics. Yet there remains room for this research area to grow. To date, most analytical readouts are optical in nature, relatively few studies have integrated sample preparation, and passive means for droplet formation and manipulation have dominated the field. Analytical scientists continue to expand capabilities by developing droplet-compatible method adaptations, for example, by interfacing to mass spectrometers or automating droplet sampling for temporally resolved analysis. In this review, we highlight recently developed fluidic control techniques and unique integrations of analytical methodology with droplet microfluidics—focusing on automation and the connections to analog/digital domains—and we conclude by offering a perspective on current challenges and future applications.

INTRODUCTION

Nearly 20 years ago, informed by prior work on the stability of monodisperse emulsions (1, 2), an early foray into droplet microfluidics by Thorsen et al. (3) came about when the researchers realized that the unique and predictable fluid physics within microfluidic channels (4) could be exploited to consistently form droplets between two immiscible fluids such as water and oil. Soon afterward, a number of studies revealed that a vast array of manipulations and novel analytical applications could be achieved with droplet microfluidics, mainly with aqueous-in-oil droplet formation. Among many other productive research groups, Ismagilov and coworkers suggested that rapid dynamics could be explored (5), the Whitesides and Stone laboratories explored device-dependent behavior (6), the Weitz group explored high-throughput analytical possibilities and multiple emulsions (2, 7), the Mathies laboratory investigated the use of valve-based automation in droplet microfluidics (8, 9), and Chiu explored precise droplet analysis with fluorescence correlation spectroscopy (10). Generally, in these and other related studies, microfluidic devices have permitted the generation of precisely defined droplets, which served as unique individual microreactors (usually picoliter or nanoliter volume) that could be processed and analyzed downstream in operations such as delivery, merging, mixing, sorting, or analysis (11).

Researchers have leveraged these populations of typically monodisperse droplets to reveal several outstanding benefits (12). The extraordinarily small volumes not only save reagents but also enable unique analyses on single cells or even single molecules (13, 14). With nearly identical droplets generated at high throughput (often kilohertz frequencies), scientists can explore biological systems and generate data sets at larger scales than previously accessible (15). Numerous biological and chemical applications were empowered by droplet microfluidics in recent years, such as single-cell genome sequencing (16), enzyme kinetics and inhibition (17), combinatorial synthesis and drug discovery (18), protein and nucleic acid quantification (19–21), and cellular secretion detection (22, 23). As such, there are numerous review articles on droplet microfluidics, and we point the readers to a recent selection having varying perspectives: a thorough review on recent advances (24), a survey of analytical techniques (25), dynamic analysis with droplets (26, 27), passive and active formation (28), droplet tracking and barcoding (29), single-cell analysis (30), tissue engineering and analysis (31), synthetic biology (32), nucleic acid cytometry (33), and drug discovery within droplets (34).

To date, most studies in droplet microfluidics have remained reliant on optical readout of droplet contents (mainly with fluorescence) owing to the method's simplicity, compatibility with microchannels, and the lack of interference from carrier fluids such as oils. Likewise, the majority of studies have also used passive fluidic features. More recently, several groups have expanded the use of active droplet formation and control using, for example, elastomeric valves, and other analytical steps such as bead-based cleanup and mass spectrometry (MS) have been integrated with droplet microfluidics. In this review, we focus on important recent developments in active or automated microfluidic flow control strategies for droplet formation and handling, and we highlight the connection to electronic concepts in digital and analog information with some example channel architectures and analytical applications.

FLOW CONTROL IN DROPLET MICROFLUIDICS

Passive Droplet Control

In a droplet-based two-phase flow microsystem, two immiscible fluids under flow or pressure regulation meet at a junction, resulting in segments of the one contained in the other that are transported downstream depending on viscous and interfacial forces (35, 36). To drive droplets in a preferred route at a desired speed, passive mechanisms can maintain this balance through

regulation of channel geometry, hydrodynamic pressures, surface hydrophilicity/hydrophobicity, viscosity of the continuous phase, and interfacial tension between the two phases (7, 15, 37). As surface tension is highly relevant, surfactants play a significant role in modulating droplet properties (1, 28, 38, 39). Several droplet generation techniques have been developed so far, exploiting different device geometries that can passively regulate droplet size in various ways. In two-phase flow microfluidics, cross-flow, coflow, and flow-focusing are three of the major generator types, named for how the phases interact with the interfaces (28, 36, 40). A number of reviews have covered passive droplet formation and maneuvering; for more detailed information, we direct readers to the thorough survey by Zhu & Wang (28) and to Dressler and coworkers' apt description of formation structures published in the 2017 volume of this journal (26).

PDMS: polydimethylsiloxane

Active Droplet Control

To realize the array of applications achieved through droplet microfluidics, precise control over the size, volume, and frequency of formed droplet is of utmost importance. While this can be accomplished passively without external actuation, active regulation provides more authority and precision, albeit at lower throughput and with additional input energy (15, 36). Device-to-device variations, ambient conditions, and surface chemistry fluctuations are example issues that cause droplet formation inconsistencies in passive systems. These issues can be largely negated by active mechanisms, which can be interfaced to a computer to give flexibly programmable droplet formation.

Active mechanisms execute different droplet operations by employing external controllers. Depending on the type of energy applied, these actuations can be classified as mechanical, electrical, thermal, or magnetic (41). Monolithic membrane valves are the most common mechanical means, as they can precisely regulate fluidic flows and mediate droplet generation and other maneuvers (22, 23, 42–49). Although a thin layer of polydimethylsiloxane (PDMS) is traditionally used to act as the valve gate, three-dimensional (3D) printing technology has recently been introduced for rapid, cost-effective production of both normally open and normally closed valves that can be actuated at low operational pressures (50–52).

Alternating current (AC) electric fields are often applied externally or within microchannels with nearby electrodes to aid in destabilizing the fluidic interface and initiating droplet generation, merging, sorting, and more operations (53, 54). The Abate group (55) described a clever approach making this method more accessible, where a concentrated salt solution in a microchannel replaced traditional metal electrodes and provided further customization of the electrode designs (49). Alternatively, electrowetting is popular for controlling the dynamics of discrete droplets by tuning its ability to wet a planar surface, a phenomenon subject to an affiliated field of study known as digital microfluidics (56–59).

Magnetic and thermal transducers are other means of active droplet coordination. A permanent magnet or an electromagnet can be used to regulate the size of droplets forming off a ferromagnetic fluid (60, 61) depending on its point of application (62), magnetization (28), and strength of the magnetic field (61). Further, the viscosity and interfacial tension of most fluids decrease fairly linearly with increasing temperature (41); thus, integrated heating can tune these properties to enable droplet operations such as thermally mediated breakup and formation (63).

Even though a larger number of off-chip controls may make the initial setup cumbersome, the automation capability of these active methods can ensure both accuracy and precision, especially in experiments that require precise volume metering or have to be operated for a longer time. For instance, our laboratory has shown that phase-locked detection can permit up to 100-fold improvements in optical limits of detection using a pair of sample and reference droplets, but to do so requires generation in an alternating pattern at very narrow bandwidth (49, 64–66). While

passive mechanisms are still far superior for high-throughput generation (28)—often one or two orders of magnitude faster compared to active methods (41)—analyses that demand quality over quantity require resorting to active means, as described herein.

FIFO: first-in first-out

μChopper: microfluidic sample chopper

ADVANCES IN FLUIDIC CONTROL AND INTERFACING

Active Systems Using Membrane Valves

The introduction of integrated membrane valving concepts in microfluidics (44, 45, 67) was followed by significant further development by the Quake (68, 69) and Mathies (44, 70) groups. Their work paved the way for a wide variety of unique and impactful microfluidic applications that are too numerous to adequately review here. Interestingly, for quite a few years, these types of valves were only sparingly used (9, 71–74) within the subfield of droplet microfluidics, perhaps due to the ease with which droplets can be formed passively. Nonetheless, work in this area has continued, and several groups have recently demonstrated unique and powerful capabilities by combining membrane structures to facilitate droplet formation and various movements.

As shown in **Figure 1*a***, the DeVoe group (47) has recently demonstrated programmable integration of droplet generators, traps, and mergers with membrane valves and strategically placed bypass channels. Various actions were accomplished on demand, such as trapping in a first-in first-out (FIFO) manner, analysis, selective ejection, merging, and sorting, and the device was applied to single-cell trapping and screening. This group then used a microfluidic multiplexer and a novel, multidepth droplet trap structure (**Figure 1*b***) to demonstrate random-access trapping and release of arrays of picoliter droplets or cells (48). Using normally open valves and pumps for droplet formation and downstream analysis, our group has shown that the precise control of droplet frequencies at narrow bandwidths allows lock-in detection for significant reductions in optical detector noise (65, 66), in a device termed the μChopper. By further combining this automation and μChopper readout with salt water merging electrodes, a fully programmable device was validated for combinatorial analysis and on-chip immunoassays (**Figure 1*c***). Although a clear disadvantage of these systems is their low droplet frequencies (~0.1–10 Hz), one notable advantage of the programmability is the extraordinary consistency with which users can regulate droplet frequency, size (volume), merging ratios, and trapping and retrieval positions.

Unique Droplet Junctions with Active Control

Typical droplet formation and handling structures are based on microchannel network designs with only two channels at each junction or node, such as the T-junction droplet generators shown in **Figure 1*a,c***. Doonan & Bailey (75) introduced a clever advancement in 2017, termed the K-channel, where multiple channels intersect at a single node interfaced to a nearby merging electrode and/or magnet (**Figure 1*d***). The elegance of this design is that cross-channel flow can be coupled to droplet flow at the intersection point, enabling multiple versatile operations with a single design feature, such as reagent injection, fluid extraction (as shown in **Figure 1*d***), droplet splitting, and magnetic bead capture. The K-channel is categorized here as active because it does require a precisely balanced flow rate in a separate liquid stream. Unlike other active structures, the K-channel operates successfully in the droplet frequency range of 200–500 Hz.

Despite the numerous advantages and potential applications of droplet microfluidics, a major limitation has been the lack of robust integration with solid-phase techniques. If these devices are to be successfully applied to solve many biochemical problems, the bottleneck of manual sample cleanup and extraction must be addressed. To attend to this need, the Bailey group (76) recently developed another unique droplet junction, the coalesce-attract-resegment wash

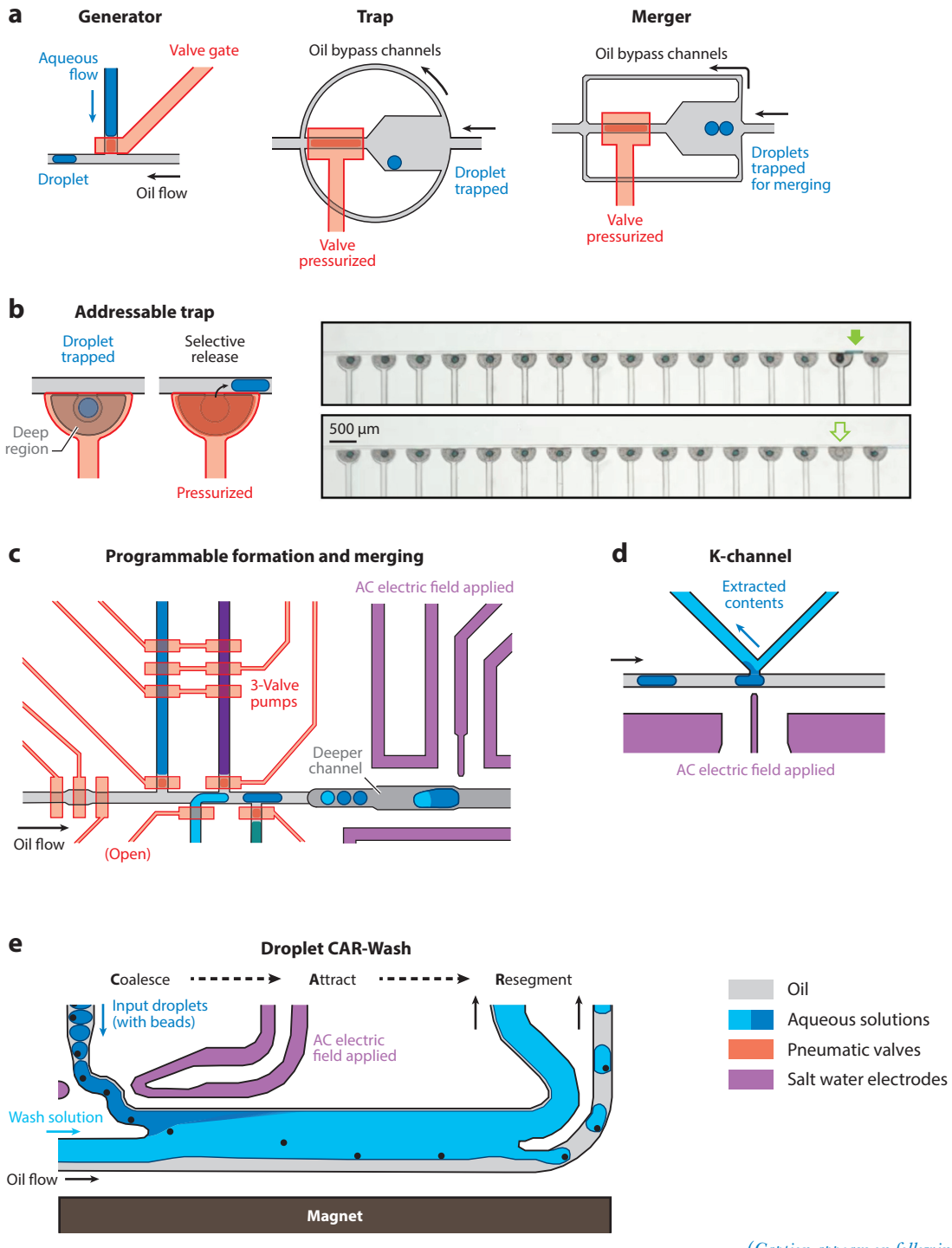

(*Caption appears on following page*)

Figure 1 (*Figure appears on preceding page*)

Recent advances in active droplet control. (*a*) Membrane valve structures for programmable generation, trapping, and merging of droplets and (*b*) addressable trapping and releasing of droplets or cells. Panel adapted with permission from Reference 47; copyright 2019 Royal Society of Chemistry; panel adapted with permission from Reference 48; copyright 2020 AIP Publishing. (*c*) Pneumatic valve-based on-chip pumps combined with salt water electrodes for programmable formation and merging of multiple droplet populations at well-controlled ratios. Panel adapted with permission from Reference 49. (*d*) The K-channel architecture enables multiple unique functions, such as selective extraction of contents (*dark blue*) into an aqueous stream (*light blue*) in real time. Panel adapted with permission from Reference 75; copyright 2017 American Chemical Society. (*e*) The coalesce-attract-resegment wash (CAR-Wash) structure for bead washing provides efficient, continuous washing of magnetic beads within droplets. Panel adapted with permission from Reference 76; copyright 2019 Royal Society of Chemistry.

(CAR-Wash) design (**Figure 1*e***). The droplet CAR-Wash structure accepts three inputs with controlled flow (bead-containing droplets segmented in oil, a wash solution, and another oil stream for resegmenting), uses two active on-chip structures (salt water electrode and magnet), and outputs two streams with both aqueous and oil components (waste and resegmented droplets containing washed beads). This approach was useful at droplet frequencies above 500 Hz, it achieved 98% retention of beads, and it allowed over 100-fold dilution in the final droplets. The CAR-Wash design should enable users to integrate more sample preparation steps into on-chip droplet microfluidics workflows. One immediately obvious application could be to adapt multistep, bead-based immunoassays into segmented flow streams.

Other unique junctions have been developed recently. Shojaeian & Hardt (77) applied a controllable direct current (DC) electric field within a channel adjacent to a standard T-junction droplet generator, allowing active control over droplet sizes and sequences. Similarly, Teo et al. (78) improved upon the salt water electrode design at the droplet junction, and they used AC electric fields for on-demand size control of droplets made from both Newtonian and non-Newtonian fluids. Raveshi et al. (79) elected to use pressure-based control in an adjacent valve channel to accomplish selective droplet splitting at a downstream channel junction. They found that the size of split droplets depended strongly upon the pressure applied to the inlets and the valve, and the single-layer valve design simplified device fabrication. While this is by no means a comprehensive list, these examples highlight some creative adaptations of droplet control junctions in recent years.

Novel Optical Interfacing

Photoinitiated reactions can also be achieved actively within droplets using light sources. For example, Choi et al. (80) photo-polymerized monodisperse polyethylene glycol diacrylate (PEGDA) droplets on-chip using a UV light source integrated downstream of a cross-flow droplet generator. Because PEGDA polymerization is strongly inhibited by oxygen molecules consuming photoinitiated free radicals, Oakey's group (81) introduced a stream of nitrogen gas that was able to purge the system, offering better control over microsphere size and uniformity. Di Carlo and coworkers (82) increased both scalability and throughput in microgel production using pH adjustments and an oil-soluble organic base. The same group also used coordinated polymerization to fabricate "dropicles," uniform particles that template aqueous-in-oil compartment formation (83); these particles have significant potential owing to their ability to form compartments without fluidic channels. By integrating an optical waveguide, mirror, droplet formation, and bead suspension hopper structures on-chip, Paegel and coworkers (18) developed the *hν*SABR (light-induced and -graduated high-throughput screening after bead release) architecture (**Figure 2*a***). Accurate photochemical reaction dosing was possible with this system, and beads displaying photochemically cleavable pepstatin A were used for dose-response screening in an HIV-1 protease activity assay.

Droplet CAR-Wash: droplet coalesce-attract-resegment wash

PEGDA: polyethylene glycol diacrylate

***hν*SABR:** light-induced and -graduated high-throughput screening after bead release

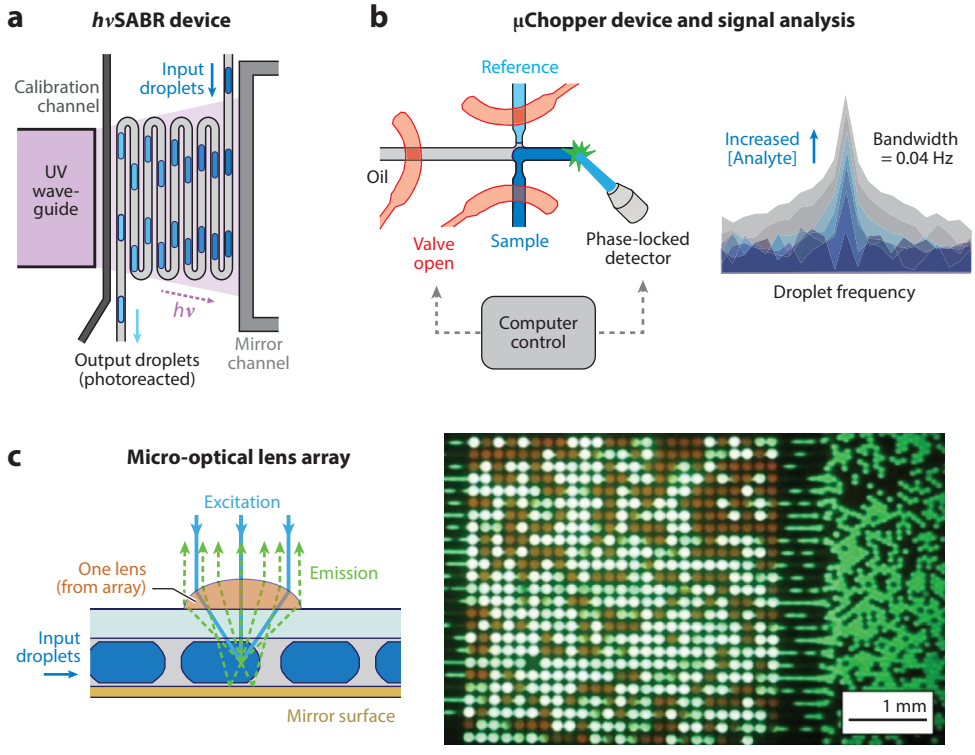

Figure 2

Unique interfaces of droplets with light sources. (*a*) Photoinitiated reaction management within droplets using integrated on-chip structures by Paegel and coworkers. Panel adapted with permission from Reference 18; copyright 2016 American Chemical Society. (*b*) By locking in the detection and valving systems, our group has shown up to a 100-fold noise reduction with the μChopper device. Panel adapted with permission from Reference 65; copyright 2017 American Chemical Society. (*c*) Baret and coworkers designed a micro-optical lens array for high-throughput fluorescence emission measurements. Panel adapted with permission from Reference 84; copyright 2013 Royal Society of Chemistry. Abbreviations: *hν*SABR, light-induced and -graduated high-throughput screening after bead release; UV, ultraviolet.

Optical detection is widely used for measuring droplet contents in microfluidics, with fluorescence most commonly employed. Absorbance detection has been applied, but the fundamental dependence on optical path length becomes limiting in micrometer channel dimensions. In fact, weak optical signals of any type require more elaborate optics or phase-locked detectors to efficiently improve sensitivity. Recognizing that droplet formation is essentially "chopping" the fluidic sample, our group exploited this inherent nature of droplet formation as a microfluidic sample chopper—termed the μChopper—an analog to the optical beam chopper (64). Absorbance detection limits were improved by more than 100-fold without modifying optics. Similarly, using continuous illumination while locking in the optical detector to the frequency and phase of droplet forming valves, we showed over 50-fold noise reduction in fluorescence (49, 65, 66) (**Figure 2*b***). The uptake rate of free fatty acids in single 3T3-L1 adipocyte cells was quantified for the first time as $3.5 \pm 0.2 \times 10^{-15}$ mol cell^{-1}, and the mass detection limit of insulin using in-droplet homogeneous immunoassays was 2×10^{-16} mol. Because precise frequency regulation provides significant enhancements in this system, this device in particular—with 0.04-Hz

bandwidth in droplet formation—highlights the fact that the integration of computer-controlled valves with droplet microfluidics can facilitate new analytical capabilities.

Another unique optical interface involves arrays of small lenses matched to the droplet detection spots. The Baret group (84) showed that a micro-optical lens array (**Figure 2*c***) could be used for massively parallel droplet detection, with throughputs of ~2,000 droplets s^{-1} and per lens, and with over 625 measurement points. Later, the deMello group (85) validated their version of a microlens array by analyzing 50,000 cells s^{-1}. The same research group (86) later used a counter-propagating lens/mirror system that enhanced signals by two orders of magnitude while also analyzing up to 40,000 droplets s^{-1}. These microlens array systems are particularly powerful and efficient, as they can be microfabricated and matched to the dimensions of the microchannels.

Oil Draining and Aqueous/Oil Separators

From injecting reagents to detecting analytes, droplets under operation require enough spacing in sequence to avoid undesired coalescence or content leakage and to assist detection. Obviously, the oil carrier plays an important role here. While gas bubbles and liquid plugs have been used as spacers, these introduce more complexity (87). The reverse operation to spacing is oil drainage, which is often leveraged to help merge adjacent droplets. Lee et al. (88) utilized a drainage channel with smaller dimensions than the main channel to draw off the oil spacers between droplets before electric field-based coalescence. The Bailey group (89) recently applied two counter-flowing oil streams to help remove oil spacing in real time, a device named the counter-current continuous phase extraction (C^3PE) module that was capable of processing at 40–200 Hz.

Droplet generators are often coupled with various analytical tools to detect, screen, or investigate. Some schemes require droplets to be completely separated from their oil carrier prior to analysis to ensure maximum throughput and minimum interference (90, 91). Many separation methods involve transferring the droplets from their oil carrier to an aqueous stream—in a parallel flow of the two—with the aid of a modified hydrophilic surface or an applied electric field, as in the CAR-Wash structure (**Figure 1*e***) (76). Fidalgo et al. (90) and the Kennedy group (91, 92) have used similar aqueous/oil separators, which are discussed in detail later. Some other separation techniques have drained the oil while retaining droplets by employing geometric obstacles on the flow path (93), creating hydrophobic side channels (94, 95), and introducing an oil-absorbing membrane on an extraction interface to couple to electrophoresis (96).

FLUIDIC ANALOG-TO-DIGITAL OPERATIONS USING DROPLETS

Readers with a background in analytical chemistry, in particular, may quickly draw comparisons between droplet microfluidics devices and the flow injection analysis (FIA) systems developed in the 1970s (97, 98). While this analogy is sound, an important distinction of droplet microfluidics is the ability to sample from a fluid stream and then essentially shut down diffusion and dispersion (5, 99) between adjacently sampled droplets. Where diffusion and dispersion are expected in FIA and are folded into the data analysis, droplet microfluidics minimizes longitudinal dispersion after segmentation, where mixing can only occur within each individual droplet through chaotic advection. Separated droplet segments are effectively chemically segregated from each other, unless some components are able to partition into the oil phase (100). As long as oil partitioning is regulated or is negligible at the experimental timescales, this spatial separation of chemical and biochemical components opens new potential applications in analytical and bioanalytical chemistry, where analogies to digital information processing are often more appropriate (22, 23, 27). In this section, we discuss the implications of droplet segmentation in the temporal analysis and control of fluidic streams and accompanying analyte signals. Moving forward, we refer to

devices that continuously sample a fluidic stream and segment it into droplets as microfluidic analog-to-digital converters (μADCs) (**Figure 3*a***); conversely, devices that start with segmented flow and generate well-controlled patterns in the output continuous flow stream are referred to as microfluidic digital-to-analog converters (μDACs) (**Figure 3*b***).

μADC: microfluidic analog-to-digital converter

μDAC: microfluidic digital-to-analog converter

Microfluidic Analog-to-Digital Conversion

Some of the earliest research in this microfluidics subfield recognized the power of droplet-based segmentation in preserving temporal dynamics of the system under study (5). One classic example is a device termed the chemistrode (101) (**Figure 3*c***). This device used segmented flow streams as both the input and the output to an external system such as cells on a glass surface. The pioneering work proved that a dynamically varying system could be fluidically sampled at short timescales and then analyzed by immunoassays, fluorescence readout, and MS. Similarly, early work by Easley et al. (102) showed that continuous droplet sampling could be used for secretion sampling from pancreatic islets with 1.9-s resolution, revealing two major classes of oscillations in secreted zinc (periods at ∼20–40 s and ∼5–10 min). In other concurrent work, Kennedy's group (103) coupled microdialysis sampling with droplet segmentation to preserve temporal resolution, and droplets were coalesced into a continuous stream and fed into a microchip electrophoresis device to evaluate glutamate and aspartate release in the striatum of living, anesthetized rats.

These systems—introduced just over a decade ago—can be fundamentally viewed as μADCs (**Figure 3*a***). A system of interest that varies dynamically over time can be sampled with nanoliter or picoliter volume droplets, and the aqueous-in-oil segmentation will prevent diffusion and dispersion from compromising the temporal record within the fluid. Importantly, the fluidic sampling resolution, Δt, will ultimately define the achievable measurement resolution downstream, and this is particularly true if the measurement requires mixing with assay reagents prior to readout. By coupling this type of μADC system to the actively controlled merging structures shown in **Figure 1*a,c,d***, researchers can preserve the temporal resolution by mixing with assay reagent droplets downstream of the sampling site (49), and essentially unlimited numbers of operations (albeit with dilution) could be carried out on the droplets downstream without detriment to Δt. Thus, by treating each sampled droplet as a snapshot in time of the chemical and biochemical information emerging from the system of interest, we have a fluidic system analogous to ADC digital circuitry. Conversely, with continuous flow, much of the temporal information from the system can be lost to diffusion and dispersion in the sampling channel, and any subsequent operations will further compromise and increase Δt (**Figure 3*a***, *right*).

Two examples of μADC fluidic architectures are shown in **Figure 3**, namely the chemistrode (101) (**Figure 3*c***) developed by the Ismagilov group and the valve-automated μADC device developed by our group for tissue secretion sampling and downstream quantitative analysis (22, 23) (**Figure 3*d***). As shown in **Figure 3*d***, automated valve-controlled segmented flow allows the time difference between droplets (Δt) to be precisely regulated, and the fluidically digitized time record can be stored downstream in an incubation channel (**Figure 3*d***, *inset*) akin to digital data storage on a hard disk.

Applications of μADCs

Novel chemical and biochemical information has been uncovered through the application of such μADC systems (**Figure 4**). In one example, a microdialysis-based neural probe μADC system developed by Petit-Pierre and coworkers (104) combined a microfluidic droplet generator with recording and stimulation electrodes. They positioned the droplet generator within 170 μm of the sampling inlet so that the resolution (Δt) was only a few seconds (**Figure 4*a***), and the

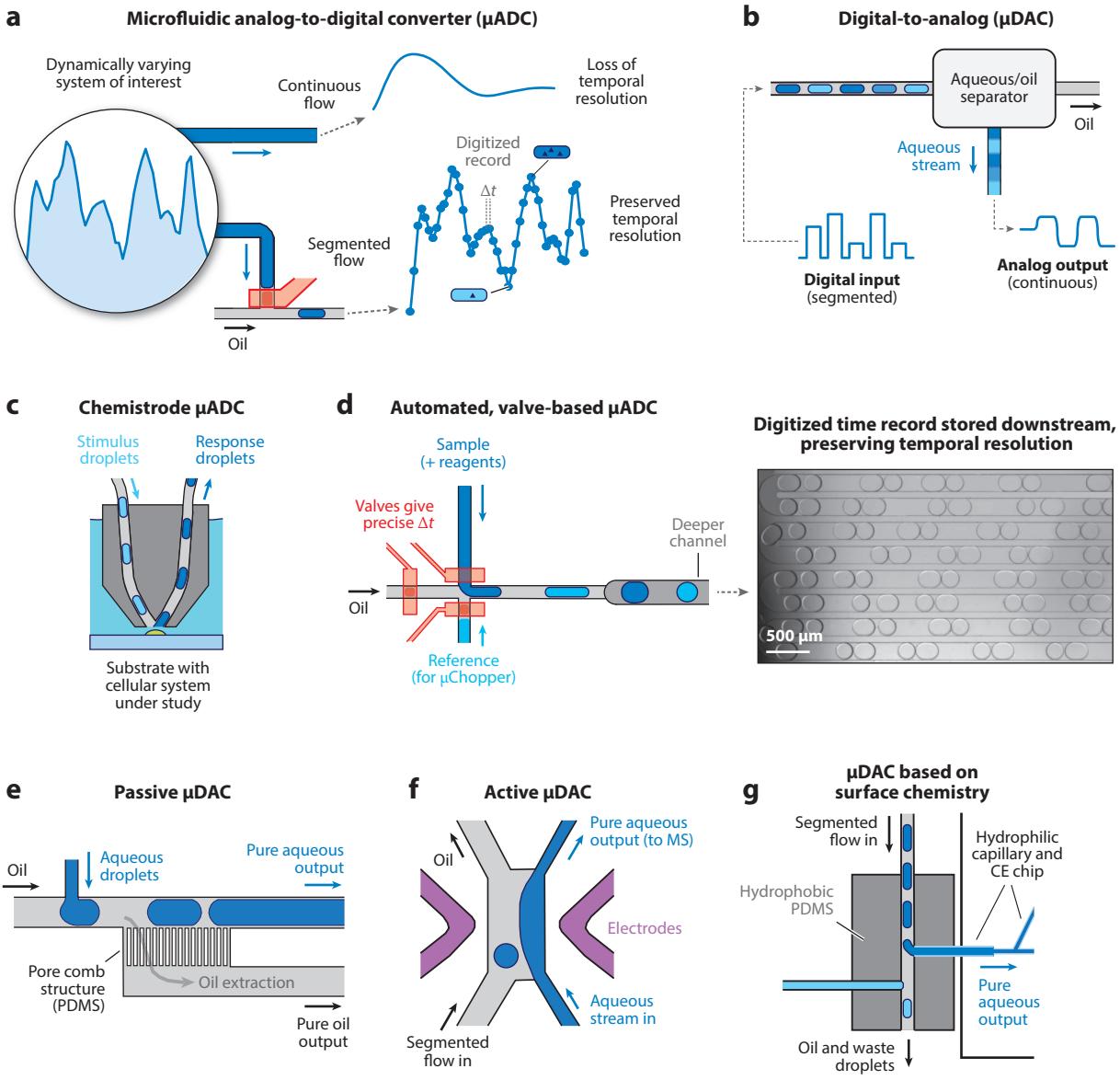

Figure 3

Concepts and fluidic designs for microfluidic analog-to-digital converter (μADC) and digital-to-analog converter (μDAC) using droplets. (*a*) Concept of μADC, where dynamic information lost in continuous flow systems is preserved at high temporal resolution (Δt) using droplet microfluidics. (*b*) Concept of μDAC, where trains of input droplets can be coalesced and separated from oil to provide a high-resolution continuous aqueous stream with concentrations defined by the input droplet train. (*c*) Fluidic design of the chemistrode device, also a μADC. Panel adapted with permission from Reference 101; copyright 2008 National Academy of Sciences. (*d*) Automated, computer-controlled valves give highly consistent Δt, and fluidic digitization can be stored downstream as digital data (*right*). Panel adapted with permission from Reference 22; copyright 2018 Royal Society of Chemistry. (*e*) Fluidic design of a passive aqueous/oil separator that converts digitized fluidics into a continuous stream to serve as a μDAC. Panel adapted with permission from Reference 94; copyright 2010 American Chemical Society. (*f*) Active μDAC design based on dielectrophoretic merging of a droplet train with a flowing aqueous stream, interfaced with mass spectrometry. Panel adapted with permission from Reference 90; copyright 2009 Wiley. (*g*) μDAC using surface wettabilities to separate oil and aqueous streams. Panel adapted with permission from Reference 91; copyright 2014 American Chemical Society. Abbreviations: CE, capillary electrophoresis; MS, mass spectrometer; PDMS, polydimethylsiloxane.

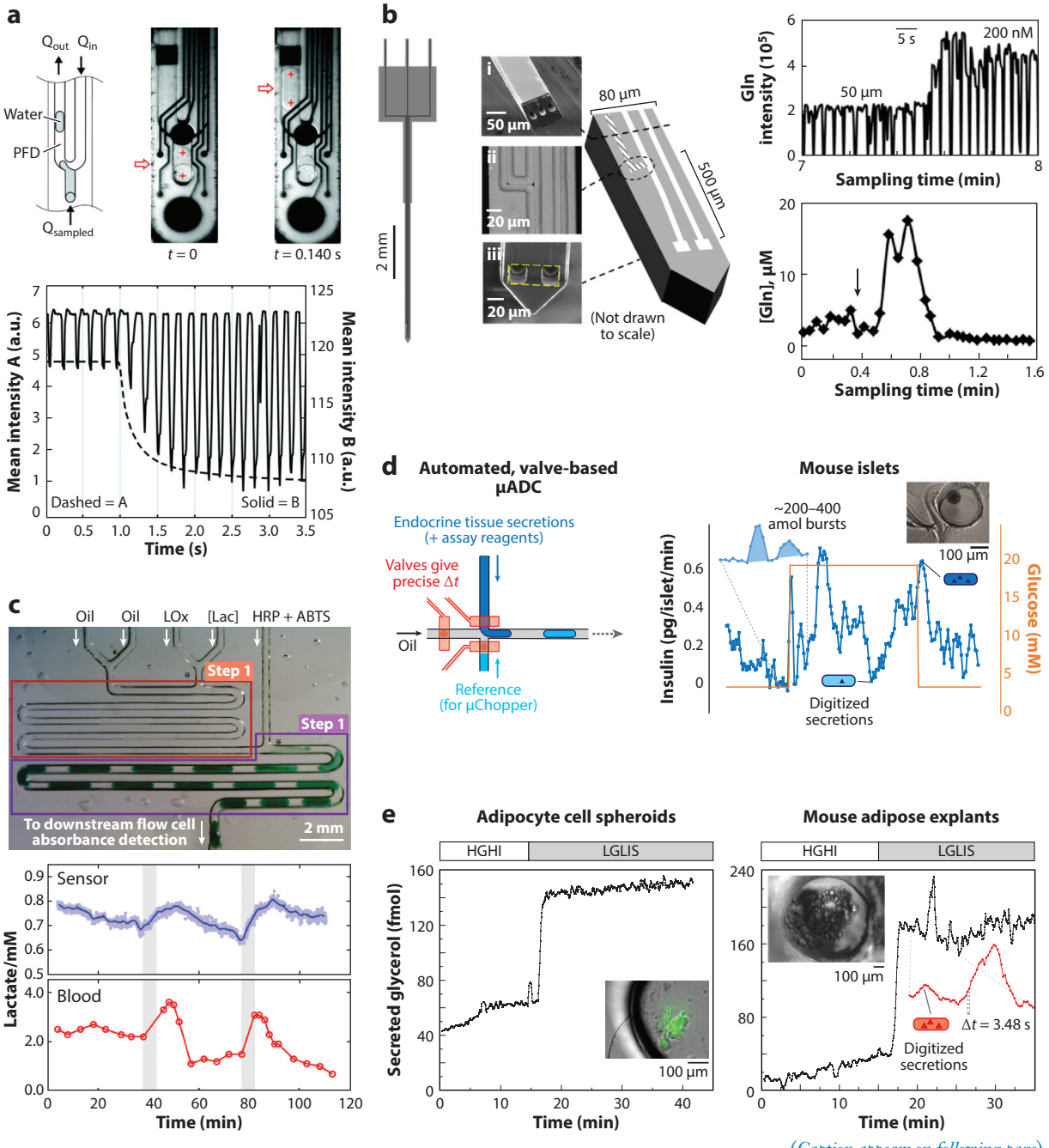

(Caption appears on following page)

Figure 4 (*Figure appears on preceding page*)

Applications of microfluidic analog-to-digital converter (μADC). (*a*) Neural probe μADC with device designs at top, and analog (*dashed line*) to digital (*solid line*) data shown at bottom. Panel adapted with permission from Reference 104; copyright 2016 Royal Society of Chemistry. (*b*) Combined microfabricated push-pull probe, droplet sampling, and nESI-MS analysis for multiplexed in vivo neurotransmitter quantification at $\Delta t = 6$ s. Panel adapted with permission from Reference 106; copyright 2018 American Chemical Society. (*c*) Wearable μADC device for high-resolution analysis of glucose and lactate directly in dermal tissue. Panel adapted with permission from Reference 107 (CC BY). (*d*) Automated μADC device integrated with homogeneous insulin and glycerol assays to study pancreatic and (*e*) adipose tissues, respectively. Unique biological information was observed in both classes of ex vivo tissue explants at $\Delta t = 3.5$ s. Panel adapted with permission from References 22 and 23; copyright 2018 and 2020 Royal Society of Chemistry. Other abbreviations: ABTS, 2,2′-azino-bis(3-ethylbenzothiazoline-6-sulfonic acid); Gln, ^{13}-C glutamine; HGHI, high glucose, high insulin; HRP, horseradish peroxidase; Lac, lactate; LGLIS, low glucose, low insulin, with isoproterenol; LOx, lactate oxidase; nESI-MS, nanoelectrospray ionization–mass spectrometry; PFD, perfluoromethyldecalin.

engineered probe (**Figure 4*a***, *top*) was validated for translating from an analog stream to digital fluid segments at high temporal resolution (**Figure 4*a***, *bottom*). This system was later applied to monitor neurochemical dynamics in rat brains in vivo at a resolution of 50 s (105). The Kennedy group (106) has also made measurements in vivo by combining a microfabricated push-pull probe integrated with droplet-based sampling (**Figure 4*b***). The small probe size permitted a 1,000-fold improvement in spatial resolution, and droplet-based segmentation close downstream allowed 6-s temporal sampling resolution (Δt) at low perfusion rates. Impressively, they also coupled the system to nanoelectrospray ionization–mass spectrometry (nESI-MS) for simultaneous determination of glutamine, glutamate, γ-aminobutyric acid, and acetylcholine, revealing rapid in vivo neurochemical release times of 15 s in the brains of live rats following potassium stimulation. **Figure 4*b*** shows scanning electron microscopy (SEM) images of the probe, with fluidic μADC test data on the top right and in vivo data at the bottom right, both showing high-resolution glutamine quantification by MS. Nightingale et al. (107) recently demonstrated an impressive in vivo application with their wearable μADC device. Droplet sampling was integrated into this wearable sensor to quantify glucose and lactate directly in dermal tissue (**Figure 4*c***).

Our laboratory has applied an automated, valve-based μADC device (**Figure 3*d***) for sampling and quantification of secretions from endocrine tissue explants. Building from earlier work with a passive sampler (102), we first applied our automated μADC to murine pancreatic islet tissue (22). Small-volume, droplet-compatible homogeneous immunoassays were developed for insulin (108), and these reagents were mixed upstream of droplet formation using on-chip pumps (**Figure 4*d***). Because we used the μChopper concept (49, 64–66), highly sensitive insulin quantification was accomplished by simple optical measurements on-chip with a standard fluorescence microscope. This device revealed insulin secretion oscillations upon glucose stimulation (**Figure 4*d***, *right*), with timing that matched with calcium oscillations, and rapid insulin bursts in the range of hundreds of attomoles were observed quantitatively for the first time. The device was recently updated to include more assay reagent channels, and a coupled enzyme assay for glycerol was integrated (23) and used to study the differences between adipocyte spheroids (cultured cells) and ex vivo adipose tissue from mice. High-resolution data ($\Delta t = 3.48$ s) on glycerol secretion showed that rapid lipolytic oscillations were present in adipose tissue (**Figure 4*e***, *right*) but not in the cell spheroids (**Figure 4*e***, *left*). These previously unreported glycerol oscillations occurred at frequencies of 0.2 to 2.0 min^{-1}, with low-level bursts (~50 fmol) released in basal conditions and larger bursts (~300 fmol) during stimulation. The application showed that high-resolution, quantitative sampling using our μADC device enabled observation of the unique biological information concerning cellular connectivity. This analytical framework should be well suited for future studies of dynamic oscillatory function in various other tissues.

nESI-MS: nanoelectrospray ionization–mass spectrometry

Microfluidic Digital-to-Analog Conversion

Devices that use the reverse operation begin with a segmented flow stream, i.e., a digital input, then separate the aqueous and oil phases into individual streams (analog output). These devices can be viewed as μDACs (**Figure 3*b***). In this way, users can essentially program a dynamically varying signal into a segmented stream of nanoliter or picoliter volume droplets, and the μDAC will output a dynamically varying aqueous stream with precise changes defined by the input droplets with high temporal resolution (also defined as Δt).

MCE: microchip capillary electrophoresis

Many of the early works discussed above concerning droplet mergers or aqueous/oil separators, while not explicitly described this way in the publications, fit the description of μDAC use. Angelescu et al. (94) showed that a passive aqueous/oil separator could be made using the native substrate (PDMS) surface chemistry and channel aspect ratios. The oil stream easily flowed downward (**Figure 3*e***) through narrow channels, while the aqueous stream was driven forward, providing μDAC operation. This group also used oil-wet fluoropolymer membranes to instead retrieve the oil phase. A similar oil draining method was used by Ostromohov et al. (95), who created the highest-resolution μDAC to our knowledge ($\Delta t = 0.56$ s; 1.8 Hz) (see **Figure 5*b***). Using dielectrophoresis with high AC voltages applied to on-chip electrodes, Fidalgo et al. (90) demonstrated that a stream of segmented droplets could be coalesced with a continuous aqueous stream and later coupled to MS analysis (**Figure 3*f***). Also using surface chemistry and oil/droplet wetting behavior to their advantage, the Kennedy group (91) separated oil and aqueous solution at a T-junction (**Figure 3*g***). In this device, a segmented flow input was converted to continuous streams of oil and aqueous solution, thereby functioning as a μDAC device that continuously injected samples into a microchip capillary electrophoresis (MCE) channel. They later designed a modified device that interfaced droplet inputs to both MCE and gel electrophoresis on-chip (109), studying protein–protein interactions and enzyme samples at 10 s per sample, and over 1,000 separations were done before device reconditioning was necessary. One can imagine a variety of possibilities in applying these types of fluidic architectures (μDAC devices), and several example applications are discussed in detail below.

Applications of μDACs

A number of unique applications have been accomplished using the aforementioned devices (**Figure 5**). In one example, using the μDAC device concept shown in **Figure 3*g***, Guetschow et al. (91) sampled a library of potential enzyme activity modulators from multiwell plates, segmented these into 8-nL aqueous-in-oil droplets (digital information), and introduced the droplets into an MCE device capable of subsecond separation times. **Figure 5*a*** shows their excellent example of μDAC operation, where a digital input (**Figure 5*a***, *black*, *top*) is translated to an analog output (**Figure 5*a***, *red*, *top*). Driven by the digital droplet input, this device output a continuous stream of subsecond mobility shift assays of protein kinase A activity, and 96 samples were analyzed in only 12 min with minimal sample input. The middle data set shows 10 rapid MCE electropherograms and the response to increasing rhodamine (R) in subsequent droplets, while the bottom data set shows electrophoresis peak areas of rhodamine), substrate, and product during analysis of 12 samples (2 controls, 10 test compounds). This example highlights the power of combining droplet-based microfluidics with rapid MCE, where the analytical benefits of rapid analysis, very low sample consumption, and high-throughput screening are combined into one integrated device.

Ostromohov et al. (95) used their high-resolution μDAC device ($\Delta t = 0.56$ s) to deliver sequential reagents with minimal dispersion to a surface. **Figure 5*b*** (*top*) shows fluorescence images

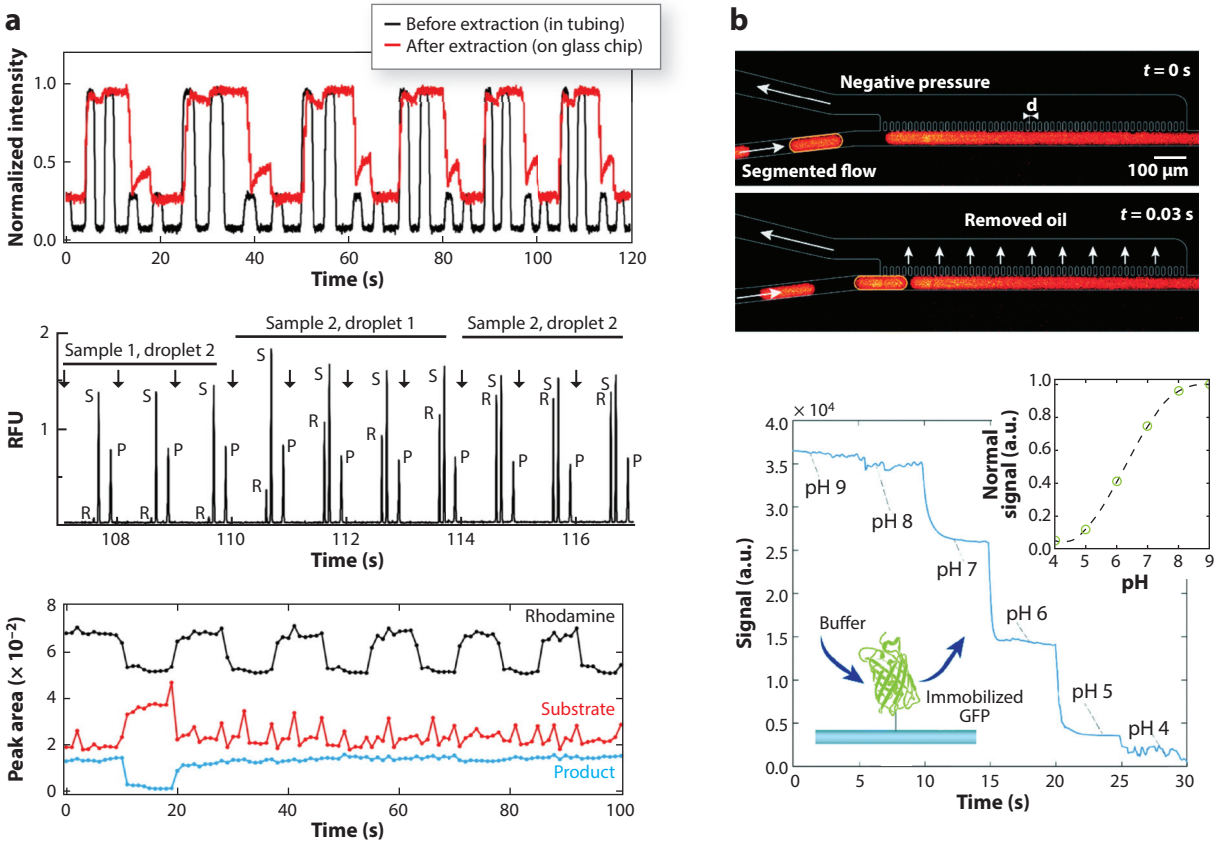

(*Caption appears on following page*)

Figure 5 (*Figure appears on preceding page*)

Applications of the microfluidic digital-to-analog converter (μDAC) using droplets. (*a*) Interfacing a μDAC device to inject a stream of nanoliter samples directly into subsecond mobility shift assays of protein kinase A activity. Panel adapted with permission from Reference 91; copyright 2014 American Chemical Society. (*b*) A high-resolution μDAC (temporal resolution, $\Delta t = 0.56$ s) was validated by rapidly inducing changes to surface green fluorescent protein (GFP) fluorescence. Panel adapted with permission from Reference 95; copyright 2016 Royal Society of Chemistry. (*c*) Mass-activated droplet sorting (MADS), where an input droplet train was split and passed to a μDAC for electrospray ionization–mass spectrometry (ESI-MS) interfacing while simultaneously sorting with dielectrophoresis. Panel adapted with permission from Reference 110; copyright 2020 Wiley. Other abbreviation: RFU, relative fluorescence units.

of the device in operation, where digitized segmented flow is translated to a continuous aqueous stream using a wettability filter. One application of the device was to modify the fluorescence emission of surface-immobilized green fluorescent protein (GFP) by rapid pH changes in the μDAC-delivered buffer (**Figure 5*b***, *bottom*). The Inglis group (111) developed a similar needle-like μDAC device to translate segmented flow through hydrophilic capillaries, resulting in a continuous stream of solution to a surface at a chemical signal response time of ∼3 s. This research group has published a recent review of literature on the dynamic transport of chemical signals using droplets, which the readers may find especially informative and complementary to this review (27).

Finally, we chose to highlight one of the most powerful analytical applications of droplet-based microfluidics to date: the mass-activated droplet sorting (MADS) device (110). This device integrates multiple droplet-handling features, of which a μDAC device is merely one. As shown in **Figure 5*c***, a previously formed emulsion of droplet-encapsulated library components is reinjected into the device, then a splitter breaks each droplet into two daughter droplets at a 4:1 volume ratio. The larger daughter droplets are diverted to an exit leading to an ESI-MS interface; this is the μDAC part of the device because the ESI-MS requires continuous aqueous input. Meanwhile, the sequence of smaller daughter droplets is fed into a delay line to wait for MS data. Lastly, a DEP-based sorting module is used to sort the smaller droplets based on the MS signal from its corresponding larger droplet. The MADS technique is able to use MS to sort thousands of droplets at 0.7 samples s^{-1} (∼15,000 samples in 6 h). The method was ultimately used to directly detect a substrate of a transaminase, 1-(imidazo[2,1-b]thiazol-6-yl)propan-2-amine (ATA Substrate) for screening the activity of the enzyme via in vitro expression within the droplets. Since the ATA Substrate and the products are not distinguishable optically without chromatography, this MADS device represents an important new analytical tool in droplet microfluidics. Owing to its label-free nature, this method should greatly expand the applicability of droplet sorting in the future.

CONSIDERATIONS, CHALLENGES, AND FUTURE POSSIBILITIES

In this final section, we explore several of the considerations and questions that are important for those using or planning to use droplet-based microfluidics for dynamic analysis or control. We also provide a perspective on the current challenges, important aspects, and future possibilities in this area.

Questions and Considerations

MADS: mass-activated droplet sorting

First, a user must determine if high-resolution sampling or stimulation is needed for the intended application. If electronics is used as an analogy, needless oversampling of data in an ADC can be compared to wasteful oversampling of droplets with a μADC, which could overuse precious samples such as enzymes or biosensing reagents. In other words, if a dynamically varying system (**Figure 3*a***) oscillates with an average period of ∼1 h, there is no need to sample droplets from the system every second. On the other hand, if a system of interest varies much more rapidly

than droplets can be sampled, fluidic aliasing will occur, and the measurements may not be interpretable. Here, the user must update the droplet-based μADC device for sampling at a minimum of twice the frequency of the fastest changes in the observed system (the Nyquist rate). This concept extends to μDAC devices as well, such that the temporal resolution of stimulation should be carefully chosen depending on the size and timing of the system to be stimulated.

The scale of system under observation should also be carefully matched to the microfluidic droplet generator. For example, if the adipose tissue explants (<1 mm) depicted in **Figure 4*e*** were much larger, say 1 cm in diameter, glycerol secretions would take place over too large of an area, causing important dynamic information to be lost before droplets are even formed. Likewise, high-resolution chemical or biochemical patterns emitted from a μDAC should be scaled to the appropriate volume to adequately stimulate or modify a system of interest.

Oil partitioning is another important issue. Analytes or stimulants of interest, their interacting partners, or optical labels should be carefully evaluated for their potential to partition into the chosen carrier oil (100). This partitioning study should usually be carried out within the microdevice, as aqueous/oil surface area-to-volume ratios are very high in this setting. As long as the timescale of analyte portioning into oil is negligible compared to the experimental timescale, the system should be functional. In fact, with the MADS device recently developed by the Kennedy group (110), the team's original plan was to measure the ketone product of the transaminase reaction. However, the ketone was observed to transfer rapidly (with respect to the experimental timescale) between droplets, confounding the droplet sorting downstream. The team chose to analyze substrate depletion instead because their MS readout was highly flexible. If this type of solution is not accessible, it may be helpful to change the oil or surfactant used in the carrier phase. The worst-case scenario would be that the analyte is simply not measurable using droplet microfluidics, at least with resolution at the relevant timescales.

Value of Active Control

In this review, we chose to focus on actively controlled devices for an important reason. To reach their true potential, high-resolution μADC or μDAC devices should operate at a very narrow bandwidth around the intended frequency, as in the electronic counterparts. We contend that programmable, active regulation of the droplet frequency and phase is the most appropriate way to achieve narrow bandwidth. We have already shown the utility of active control with the μChopper concept (64–66) (**Figure 2*b***), and others have provided similar evidence (15, 36). Passive control can generate droplets at very high frequencies (tens of kilohertz), but the bandwidth can be broadened by device variations, environmental changes, and surface chemistry fluctuations.

Challenges and Future Possibilities

While certainly advantageous, most active droplet regulation methods mentioned in this review remain much slower (0.1–10 Hz) than their passive counterparts (1–10 kHz). Thus, there is a clear need for faster approaches to droplet formation and maneuvering while maintaining narrow bandwidth. One possible solution would be to fabricate on-chip valves with more rigid materials, and recent 3D-printed valves may help address the challenge (50–52). Alternatively, off-chip controls that operate through continuous feedback from measurements of droplet frequency may suffice.

Efforts to interface with more analytical techniques should also continue (25). Optical readout by fluorescence has been most popular, but there are still opportunities to interface rapid-readout spectrometers to interrogate droplet streams. As exemplified by the new MADS technique, the droplet fluidics/MS combination can be particularly powerful (110), and we hope to see more MS experts embrace droplet microfluidics as a compatible, enabling technology. Likewise, the droplet

CAR-Wash design (76) opens up new possibilities in high-throughput, continuous, bead-based sample preparation in droplets, which is an area that needs more attention.

CONCLUSIONS

The benefits of dynamic analysis with droplet-based microfluidics were summarized nicely by Feng et al. (27, p. 2) who remarked, "A real-time analytical chemistry lab. . .to fit inside the brain of a mouse does not exist. However, we can achieve similar analytical aims if we can digitize the liquid environment from precise locations. . .at precise times. . . ." Indeed, droplet microfluidics has provided the opportunity to do just that. In this review, we have compiled the most recent and relevant research in the context of temporal analysis with segmented flow, and we have focused on actively regulated systems. Viewing fluidic signal transformations in the context provided (μADC and μDAC), we contend that the high precision and programmable timing provided by active regulation are most ideally suited to push the field forward. Akin to electronic signal collection, maintaining narrow bandwidth in the sampling frequency is key, and this will allow improvements in noise reduction and also open the possibility of spectral mixing and demixing of input droplet "signals." Finally, while it is important to understand analogous concepts in electronics, the sheer abundance and complexity of chemical and biochemical information may lead to entirely new concepts in information processing.

DISCLOSURE STATEMENT

The authors are not aware of any affiliations, memberships, funding, or financial holdings that might be perceived as affecting the objectivity of this review.

ACKNOWLEDGMENTS

The authors would like to thank the US National Institutes of Health (NIH) for funding this work under grant number R01 DK093810. We also thank the College of Sciences and Mathematics and the Department of Chemistry and Biochemistry at Auburn University for their support.

LITERATURE CITED

1. Bibette J, Morse DC, Witten TA, Weitz DA. 1992. Stability criteria for emulsions. *Phys. Rev. Lett.* 69:2439–42
2. Umbanhowar PB, Prasad V, Weitz DA. 2000. Monodisperse emulsion generation via drop break off in a coflowing stream. *Langmuir* 16:347–51
3. Thorsen T, Roberts RW, Arnold FH, Quake SR. 2001. Dynamic pattern formation in a vesicle-generating microfluidic device. *Phys. Rev. Lett.* 86:4163–66
4. Squires TM, Quake SR. 2005. Microfluidics: fluid physics at the nanoliter scale. *Rev. Mod. Phys.* 77:977–1026
5. Song H, Tice JD, Ismagilov RF. 2003. A microfluidic system for controlling reaction networks in time. *Angew. Chem. Int. Ed.* 42:768–72
6. Garstecki P, Fuerstman MJ, Stone HA, Whitesides GM. 2006. Formation of droplets and bubbles in a microfluidic T-junction—scaling and mechanism of break-up. *Lab Chip* 6:437–46
7. Link DR, Anna SL, Weitz DA, Stone HA. 2004. Geometrically mediated breakup of drops in microfluidic devices. *Phys. Rev. Lett.* 92:054503
8. Kumaresan P, Yang CJ, Cronier SA, Blazej RG, Mathies RA. 2008. High-throughput single copy DNA amplification and cell analysis in engineered nanoliter droplets. *Anal. Chem.* 80:3522–29
9. Zeng Y, Novak R, Shuga J, Smith MT, Mathies RA. 2010. High-performance single cell genetic analysis using microfluidic emulsion generator arrays. *Anal. Chem.* 82:3183–90

10. Chiu DT. 2010. Interfacing droplet microfluidics with chemical separation for cellular analysis. *Anal. Bioanal. Chem.* 397:3179–83
11. Zhu Y, Fang Q. 2013. Analytical detection techniques for droplet microfluidics—a review. *Anal. Chim. Acta* 787:24–35
12. Belder D. 2005. Microfluidics with droplets. *Angew. Chem. Int. Ed.* 44:3521–22
13. Chiu DT, Lorenz RM. 2009. Chemistry and biology in femtoliter and picoliter volume droplets. *Acc. Chem. Res.* 42:649–58
14. Zheng F, Fu F, Cheng Y, Wang C, Zhao Y, Gu Z. 2016. Organ-on-a-chip systems: microengineering to biomimic living systems. *Small* 12:2253–82
15. Teh S-Y, Lin R, Hung L-H, Lee AP. 2008. Droplet microfluidics. *Lab Chip* 8:198–220
16. Kim SC, Clark IC, Shahi P, Abate AR. 2018. Single-cell RT-PCR in microfluidic droplets with integrated chemical lysis. *Anal. Chem.* 90:1273–79
17. Sjöström SL, Jönsson HN, Svahn HA. 2013. Multiplex analysis of enzyme kinetics and inhibition by droplet microfluidics using picoinjectors. *Lab Chip* 13:1754–61
18. Price AK, MacConnell AB, Paegel BM. 2016. *hv*SABR: photochemical dose–response bead screening in droplets. *Anal. Chem.* 88:2904–11
19. Tang MY, Shum HC. 2016. One-step immunoassay of C-reactive protein using droplet microfluidics. *Lab Chip* 16:4359–65
20. Gao R, Cheng Z, deMello AJ, Choo J. 2016. Wash-free magnetic immunoassay of the PSA cancer marker using SERS and droplet microfluidics. *Lab Chip* 16:1022–29
21. Wippold JA, Wang H, Tingling J, Leibowitz JL, de Figueiredo P, Han A. 2020. PRESCIENT: platform for the rapid evaluation of antibody success using integrated microfluidics enabled technology. *Lab Chip* 2:1628–38
22. Li X, Hu J, Easley CJ. 2018. Automated microfluidic droplet sampling with integrated, mix-and-read immunoassays to resolve endocrine tissue secretion dynamics. *Lab Chip* 18:2926–35
23. Hu J, Li X, Judd RL, Easley CJ. 2020. Rapid lipolytic oscillations in ex vivo adipose tissue explants revealed through microfluidic droplet sampling at high temporal resolution. *Lab Chip* 20:1503–12
24. Ding Y, Howes PD, deMello AJ. 2020. Recent advances in droplet microfluidics. *Anal. Chem.* 92:132–49
25. Liu W-W, Zhu Y. 2020. Development and application of analytical detection techniques for droplet-based microfluidics—a review. *Anal. Chim. Acta* 1113:66–84
26. Dressler OJ, Casadevall i Solvas X, deMello AJ. 2017. Chemical and biological dynamics using droplet-based microfluidics. *Annu. Rev. Anal. Chem.* 10:1–24
27. Feng S, Shirani E, Inglis DW. 2019. Droplets for sampling and transport of chemical signals in biosensing: a review. *Biosensors* 9:80
28. Zhu P, Wang L. 2017. Passive and active droplet generation with microfluidics: a review. *Lab Chip* 17:34–75
29. Duncombe TA, Dittrich PS. 2019. Droplet barcoding: tracking mobile micro-reactors for high-throughput biology. *Curr. Opin. Biotechnol.* 60:205–12
30. Matula K, Rivello F, Huck WTS. 2020. Single-cell analysis using droplet microfluidics. *Adv. Biosyst.* 4:28
31. Shi N, Moniruzzaman M., Easley CJ. 2020. Tissue engineering and analysis in droplet microfluidics. In *Droplet Microfluidics*, ed. C Ren, A Lee, pp. 221–58. Cambridge, UK: R. Soc. Chem.
32. Gach PC, Iwai K, Kim PW, Hillson NJ, Singh AK. 2017. Droplet microfluidics for synthetic biology. *Lab Chip* 17:3388–400
33. Clark IC, Abate AR. 2017. Finding a helix in a haystack: nucleic acid cytometry with droplet microfluidics. *Lab Chip* 17:2032–45
34. Price AK, Paegel BM. 2016. Discovery in droplets. *Anal. Chem.* 88:339–53
35. Pit AM, Duits MHG, Mugele F. 2015. Droplet manipulations in two phase flow microfluidics. *Micromachines* 6:1768–93
36. Shang L, Cheng Y, Zhao Y. 2017. Emerging droplet microfluidics. *Chem. Rev.* 117:7964–8040
37. Chabert M, Viovy J-L. 2008. Microfluidic high-throughput encapsulation and hydrodynamic self-sorting of single cells. *PNAS* 105:3191–96

38. DeJournette CJ, Kim J, Medlen H, Li X, Vincent LJ, Easley CJ. 2013. Creating biocompatible oil–water interfaces without synthesis: direct interactions between primary amines and carboxylated perfluorocarbon surfactants. *Anal. Chem.* 85:10556–64
39. Seemann R, Brinkmann M, Pfohl T, Herminghaus S. 2011. Droplet based microfluidics. *Rep. Progress Phys.* 75:016601
40. Christopher GF, Anna SL. 2007. Microfluidic methods for generating continuous droplet streams. *J. Phys. D Appl. Phys.* 40:R319–36
41. Chong ZZ, Tan SH, Gañán-Calvo AM, Tor SB, Loh NH, Nguyen N-T. 2016. Active droplet generation in microfluidics. *Lab Chip* 16:35–58
42. Au AK, Lai H, Utela BR, Folch A. 2011. Microvalves and micropumps for BioMEMS. *Micromachines* 2:179–220
43. Choi J-H, Lee S-K, Lim J-M, Yang S-M, Yi G-R. 2010. Designed pneumatic valve actuators for controlled droplet breakup and generation. *Lab Chip* 10:456–61
44. Grover WH, Skelley AM, Liu CN, Lagally ET, Mathies RA. 2003. Monolithic membrane valves and diaphragm pumps for practical large-scale integration into glass microfluidic devices. *Sens. Actuators B Chem.* 89:315–23
45. Unger MA, Chou H-P, Thorsen T, Scherer A, Quake SR. 2000. Monolithic microfabricated valves and pumps by multilayer soft lithography. *Science* 288:113–16
46. Zhang W, Lin S, Wang C, Hu J, Li C, et al. 2009. PMMA/PDMS valves and pumps for disposable microfluidics. *Lab Chip* 9:3088–94
47. Babahosseini H, Misteli T, DeVoe DL. 2019. Microfluidic on-demand droplet generation, storage, retrieval, and merging for single-cell pairing. *Lab Chip* 19:493–502
48. Babahosseini H, Padmanabhan S, Misteli T, DeVoe DL. 2020. A programmable microfluidic platform for multisample injection, discretization, and droplet manipulation. *Biomicrofluidics* 14:014112
49. Shi N, Easley CJ. 2020. Programmable μchopper device with on-chip droplet mergers for continuous assay calibration. *Micromachines* 11:620
50. Gong H, Woolley AT, Nordin GP. 2016. High density 3D printed microfluidic valves, pumps, and multiplexers. *Lab Chip* 16:2450–58
51. Dang BV, Hassanzadeh-Barforoushi A, Syed MS, Yang D, Kim S-J, et al. 2019. Microfluidic actuation via 3D-printed molds toward multiplex biosensing of cell apoptosis. *ACS Sens.* 4:2181–89
52. Lee Y-S, Bhattacharjee N, Folch A. 2018. 3D-printed Quake-style microvalves and micropumps. *Lab Chip* 18:1207–14
53. Link DR, Grasland-Mongrain E, Duri A, Sarrazin F, Cheng Z, et al. 2006. Electric control of droplets in microfluidic devices. *Angew. Chem. Int. Ed.* 45:2556–60
54. Tan SH, Semin B, Baret J-C. 2014. Microfluidic flow-focusing in AC electric fields. *Lab Chip* 14:1099–106
55. Sciambi A, Abate AR. 2014. Generating electric fields in PDMS microfluidic devices with salt water electrodes. *Lab Chip* 14:2605–9
56. Grimmer A, Wille R, eds. 2020. Introduction. In *Designing Droplet Microfluidic Networks: A Toolbox for Designers*, pp. 3–11. Cham, Switz.: Springer Int.
57. Pollack MG, Fair RB, Shenderov AD. 2000. Electrowetting-based actuation of liquid droplets for microfluidic applications. *Appl. Phys. Lett.* 77:1725–26
58. Sung Kwon C, Hyejin M, Chang-Jin K. 2003. Creating, transporting, cutting, and merging liquid droplets by electrowetting-based actuation for digital microfluidic circuits. *J. Microelectromech. Syst.* 12:70–80
59. Choi K, Ng AH, Fobel R, Wheeler AR. 2012. Digital microfluidics. *Annu. Rev. Anal. Chem.* 5:413–40
60. Kahkeshani S, Di Carlo D. 2016. Drop formation using ferrofluids driven magnetically in a step emulsification device. *Lab Chip* 16:2474–80
61. Liu J, Tan S-H, Yap YF, Ng MY, Nguyen N-T. 2011. Numerical and experimental investigations of the formation process of ferrofluid droplets. *Microfluid. Nanofluid.* 11:177–87
62. Tan S-H, Nguyen N-T, Yobas L, Kang TG. 2010. Formation and manipulation of ferrofluid droplets at a microfluidic T-junction. *J. Micromech. Microeng.* 20:045004

63. Ting TH, Yap YF, Nguyen N-T, Wong TN, Chai JCK, Yobas L. 2006. Thermally mediated breakup of drops in microchannels. *Appl. Phys. Lett.* 89:234101
64. Deal KS, Easley CJ. 2012. Self-regulated, droplet-based sample chopper for microfluidic absorbance detection. *Anal. Chem.* 84:1510–16
65. Negou JT, Avila LA, Li X, Hagos TM, Easley CJ. 2017. Automated microfluidic droplet-based sample chopper for detection of small fluorescence differences using lock-in analysis. *Anal. Chem.* 89:6153–59
66. Negou JT, Hu J, Li X, Easley CJ. 2018. Advancement of analytical modes in a multichannel, microfluidic droplet-based sample chopper employing phase-locked detection. *Anal. Methods* 10:3436–43
67. Ismagilov RF, Rosmarin D, Kenis PJA, Chiu DT, Zhang W, et al. 2001. Pressure-driven laminar flow in tangential microchannels: an elastomeric microfluidic switch. *Anal. Chem.* 73:4682–87
68. Thorsen T, Maerkl SJ, Quake SR. 2002. Microfluidic large-scale integration. *Science* 298:580–84
69. Melin J, Quake SR. 2007. Microfluidic large-scale integration: the evolution of design rules for biological automation. *Annu. Rev. Biophys. Biomol. Struct.* 36:213–31
70. Jensen EC, Grover WH, Mathies RA. 2007. Micropneumatic digital logic structures for integrated microdevice computation and control. *J. Microelectromech. Syst.* 16:1378–85
71. Zeng S, Li B, Xo Su, Qin J, Lin B. 2009. Microvalve-actuated precise control of individual droplets in microfluidic devices. *Lab Chip* 9:1340–43
72. Leung K, Zahn H, Leaver T, Konwar KM, Hanson NW, et al. 2012. A programmable droplet-based microfluidic device applied to multiparameter analysis of single microbes and microbial communities. *PNAS* 109:7665–70
73. Lin R, Fisher JS, Simon MG, Lee AP. 2012. Novel on-demand droplet generation for selective fluid sample extraction. *Biomicrofluidics* 6:024103
74. Zeng Y, Shin M, Wang T. 2013. Programmable active droplet generation enabled by integrated pneumatic micropumps. *Lab Chip* 13:267–73
75. Doonan SR, Bailey RC. 2017. K-channel: a multifunctional architecture for dynamically reconfigurable sample processing in droplet microfluidics. *Anal. Chem.* 89:4091–99
76. Doonan SR, Lin M, Bailey RC. 2019. Droplet CAR-Wash: continuous picoliter-scale immunocapture and washing. *Lab Chip* 19:1589–98
77. Shojaeian M, Hardt S. 2018. Fast electric control of the droplet size in a microfluidic T-junction droplet generator. *Appl. Phys. Lett.* 112:194102
78. Teo AJT, Yan M, Dong J, Xi HD, Fu Y, et al. 2020. Controllable droplet generation at a microfluidic T-junction using AC electric field. *Microfluid. Nanofluid.* 24:21
79. Raveshi MR, Agnihotri SN, Sesen M, Bhardwaj R, Neild A. 2019. Selective droplet splitting using single layer microfluidic valves. *Sens. Actuators B Chem.* 292:233–40
80. Choi C-H, Jung J-H, Hwang T-S, Lee C-S. 2009. In situ microfluidic synthesis of monodisperse PEG microspheres. *Macromol. Res.* 17:163–67
81. Krutkramelis K, Xia B, Oakey J. 2016. Monodisperse polyethylene glycol diacrylate hydrogel microsphere formation by oxygen-controlled photopolymerization in a microfluidic device. *Lab Chip* 16:1457–65
82. de Rutte JM, Koh J, Di Carlo D. 2019. Scalable high-throughput production of modular microgels for in situ assembly of microporous tissue scaffolds. *Adv. Funct. Mater.* 29:1900071
83. Destgeer G, Ouyang M, Wu CY, Di Carlo D. 2020. Fabrication of 3D concentric amphiphilic microparticles to form uniform nanoliter reaction volumes for amplified affinity assays. *Lab Chip* 20:3503–14
84. Lim J, Gruner P, Konrad M, Baret J-C. 2013. Micro-optical lens array for fluorescence detection in droplet-based microfluidics. *Lab Chip* 13:1472–75
85. Holzner G, Du Y, Cao X, Choo J, deMello AJ, Stavrakis S. 2018. An optofluidic system with integrated microlens arrays for parallel imaging flow cytometry. *Lab Chip* 18:3631–37
86. Cao X, Du Y, Küffner A, Van Wyk J, Arosio P, et al. 2020. A counter propagating lens-mirror system for ultrahigh throughput single droplet detection. *Small* 16:1907534
87. Chen X, Ren CL. 2017. A microfluidic chip integrated with droplet generation, pairing, trapping, merging, mixing and releasing. *RSC Adv.* 7:16738–50
88. Lee M, Collins JW, Aubrecht DM, Sperling RA, Solomon L, et al. 2014. Synchronized reinjection and coalescence of droplets in microfluidics. *Lab Chip* 14:509–13

89. Doonan SR, Lin M, Lee D, Lee J, Bailey RC. 2020. C3PE: counter-current continuous phase extraction for improved precision of in-droplet chemical reactions. *Microfluid. Nanofluid.* 24:50
90. Fidalgo LM, Whyte G, Ruotolo BT, Benesch JLP, Stengel F, et al. 2009. Coupling microdroplet microreactors with mass spectrometry: reading the contents of single droplets online. *Angew. Chem. Int. Ed.* 48:3665–68
91. Guetschow ED, Steyer DJ, Kennedy RT. 2014. Subsecond electrophoretic separations from droplet samples for screening of enzyme modulators. *Anal. Chem.* 86:10373–79
92. Pei J, Nie J, Kennedy RT. 2010. Parallel electrophoretic analysis of segmented samples on chip for high-throughput determination of enzyme activities. *Anal. Chem.* 82:9261–67
93. Niu XZ, Zhang B, Marszalek RT, Ces O, Edel JB, et al. 2009. Droplet-based compartmentalization of chemically separated components in two-dimensional separations. *Chem. Commun.* 41:6159–61
94. Angelescu DE, Mercier B, Siess D, Schroeder R. 2010. Microfluidic capillary separation and real-time spectroscopic analysis of specific components from multiphase mixtures. *Anal. Chem.* 82:2412–20
95. Ostromohov N, Bercovici M, Kaigala GV. 2016. Delivery of minimally dispersed liquid interfaces for sequential surface chemistry. *Lab Chip* 16:3015–23
96. Niu X, Pereira F, Edel JB, de Mello AJ. 2013. Droplet-interfaced microchip and capillary electrophoretic separations. *Anal. Chem.* 85:8654–60
97. Ružička J, Hansen EH. 1975. Flow injection analyses: part I. A new concept of fast continuous flow analysis. *Anal. Chim. Acta* 78:145–57
98. Stewart KK, Beecher GR, Hare PE. 1976. Rapid analysis of discrete samples: the use of nonsegmented, continuous flow. *Anal. Biochem.* 70:167–73
99. Tice JD, Song H, Lyon AD, Ismagilov RF. 2003. Formation of droplets and mixing in multiphase microfluidics at low values of the reynolds and the capillary numbers. *Langmuir* 19:9127–33
100. Gruner P, Riechers B, Semin B, Lim J, Johnston A, et al. 2016. Controlling molecular transport in minimal emulsions. *Nat. Commun.* 7:10392
101. Chen D, Du W, Liu Y, Liu W, Kuznetsov A, et al. 2008. The chemistrode: a droplet-based microfluidic device for stimulation and recording with high temporal, spatial, and chemical resolution. *PNAS* 105:16843–48
102. Easley CJ, Rocheleau JV, Head WS, Piston DW. 2009. Quantitative measurement of zinc secretion from pancreatic islets with high temporal resolution using droplet-based microfluidics. *Anal. Chem.* 81:9086–95
103. Wang M, Roman GT, Perry ML, Kennedy RT. 2009. Microfluidic chip for high efficiency electrophoretic analysis of segmented flow from a microdialysis probe and in vivo chemical monitoring. *Anal. Chem.* 81:9072–78
104. Petit-Pierre G, Bertsch A, Renaud P. 2016. Neural probe combining microelectrodes and a droplet-based microdialysis collection system for high temporal resolution sampling. *Lab Chip* 16:917–24
105. Petit-Pierre G, Colin P, Laurer E, Déglon J, Bertsch A, et al. 2017. In vivo neurochemical measurements in cerebral tissues using a droplet-based monitoring system. *Nat. Commun.* 8:1239
106. Ngernsutivorakul T, Steyer DJ, Valenta AC, Kennedy RT. 2018. *In vivo* chemical monitoring at high spatiotemporal resolution using microfabricated sampling probes and droplet-based microfluidics coupled to mass spectrometry. *Anal. Chem.* 90:10943–50
107. Nightingale AM, Leong CL, Burnish RA, Hassan S-U, Zhang Y, et al. 2019. Monitoring biomolecule concentrations in tissue using a wearable droplet microfluidic-based sensor. *Nat. Commun.* 10:2741
108. Hu J, Easley CJ. 2017. Homogeneous assays of second messenger signaling and hormone secretion using thermofluorimetric methods that minimize calibration burden. *Anal. Chem.* 89:8517–23
109. Ouimet CM, D'Amico CI, Kennedy RT. 2019. Droplet sample introduction to microchip gel and zone electrophoresis for rapid analysis of protein-protein complexes and enzymatic reactions. *Anal. Bioanal. Chem.* 411:6155–63
110. Holland-Moritz DA, Wismer MK, Mann BF, Farasat I, Devine P, et al. 2020. Mass activated droplet sorting (MADS) enables high-throughput screening of enzymatic reactions at nanoliter scale. *Angew. Chem. Int. Ed.* 59:4470–77
111. Feng S, Liu G, Jiang L, Zhu Y, Goldys EM, Inglis DW. 2017. A microfluidic needle for sampling and delivery of chemical signals by segmented flows. *Appl. Phys. Lett.* 111:183702